

## Phase-Matched Frequency Doubling at Photonic Band Edges: Efficiency Scaling as the Fifth Power of the Length

Y. Dumeige, I. Sagnes, P. Monnier, P. Vidakovic, I. Abram, C. Mériaud, and A. Levenson  
*Laboratoire de Photonique et de Nanostructures (CNRS UPR 20), Route de Nozay, 91460 Marcoussis, France*  
(Received 9 November 2001; published 3 July 2002)

By exploiting the unique properties of periodic stratified media we demonstrate simultaneously phase matching and enhancement of the optical field under second order nonlinear interaction. This leads to a second harmonic efficiency growth faster than the fifth power of the structure length, far better than the usual quadratic behavior associated with second order nonlinear effects.

DOI: 10.1103/PhysRevLett.89.043901

PACS numbers: 42.70.Qs, 42.65.Ky

Stratified media have been proposed in second order nonlinear optics very early in the history of that field as a means of matching the phase velocities of the waves under nonlinear interaction, in order to obtain an efficient frequency conversion. In that proposal, now referred to as quasi-phase matching, a periodic distribution of the  $\chi^{(2)}$  nonlinear susceptibility was produced in a material with uniform refractive index [1]. This periodic grating rephases the nonlinear polarization and the generated waves. An alternative method for obtaining phase matching exploits the dispersive properties of a medium with a periodic distribution of its refractive index [2]. Under particular conditions, this periodicity leads to a decrease of the group velocity of the interacting waves. This property was exploited to enhance the second harmonic generation (SHG) [3,4].

Thanks to a recent conceptual breakthrough, *finite* 1D stratified lamellar structures with a periodic variation of the refractive index have been proposed by Scalora *et al.* [5,6] for achieving simultaneously phase matching and field enhancement, thus obtaining high efficiency SHG. Periodic stratified structures present a “stop-band” that prevents light propagation within a spectral band around a central Bragg wavelength in a manner analogous to photonic band-gap structures. They are referred to by some authors as 1D photonic crystals (1D-PCs) or as distributed Bragg reflectors. The high reflectivity Bragg stop-band is surrounded by a series of relatively narrow resonances in which reflectivity drops to zero and transmission is maximal. This cancellation of reflectivity corresponds to a total phase shift of an integral value of  $\pi$  for a transmitted propagation beam. This dispersion feature of 1D-PCs implies that phase matching for SHG can be achieved if the  $2n$ th lateral resonance of the second order Bragg stop-band is at exactly twice the frequency of the  $n$ th resonance of the first order stop-band. At the same time the electromagnetic field propagating in these “distributed Bragg resonances” is enhanced. A simple analytic calculation [7] within the coupled mode approximation indicates that for a long enough Bragg structure of length  $L$  the field enhancement is proportional to  $L$ , while the intensity enhancement is proportional to  $L^2$ . Since the phase-matched SHG in-

tensity grows as  $L^2$  in the course of propagation and is quadratic in the intensity of the fundamental, this implies that phase-matched SHG in 1D-PCs should grow as  $L^6$ , a spectacular difference when compared with phase-matched SHG in bulk media where it grows only as  $L^2$ .

In this Letter we present the first experimental demonstration of this attractive proposal by applying this approach to SHG in stratified III-V semiconductors. These materials have a strong nonlinear susceptibility, but cannot be phase matched in the bulk because they are isotropic.

We begin with an analysis of the potentialities of the structure that we fabricated and studied experimentally. The structure is constituted of the alternation of low and high refractive index layers ( $\text{AlO}_x$  and  $\text{AlGaAs}$ , respectively) with a period  $d$  such that the high refractive index material ( $\text{AlGaAs}$ ) displays at the same time a second order nonlinear susceptibility. Because of the group symmetry of GaAs and related compounds, the second order nonlinear processes are forbidden at normal incidence when the structure is grown in the usual [001] direction [8]. This implies that for high SHG efficiency the incidence angle should be as large as possible and corresponding polarization should be TM. In order to achieve phase matching at large incidence angles ( $\theta_i$ ), the Bragg stop-band and the lateral resonances should not vanish at large angles, a feature that requires a large refractive index contrast. Figure 1(a) gives the  $\omega(k_x)$  dispersion relation for our structures normalized to the fundamental frequency  $\omega_0$  [9]; the  $x$  direction is the intersection between the layers and the incident plane. The white area corresponds to evanescent states, the gray areas correspond to propagating ones, and the dashed lines correspond to the light line. Clearly, band gaps appear for certain ranges of optical frequency, and since they are everywhere within the light cone, the structure displays omnidirectional reflectivity [10], a feature that permits us to operate at large angles of incidence [indicated by the full line in Fig. 1(a)].

An alternative way of looking at phase matching in 1D-PCs that makes contact with phase matching in bulk is by defining an effective wave vector for the field. The wave vector can be expanded onto the  $z$  (normal to the isotropic layers) and  $x$  directions:  $\mathbf{k}^{\text{eff}} = k_x \hat{x} + k_z^{\text{eff}} \hat{z}$ .  $\mathbf{k}^{\text{eff}}$  means

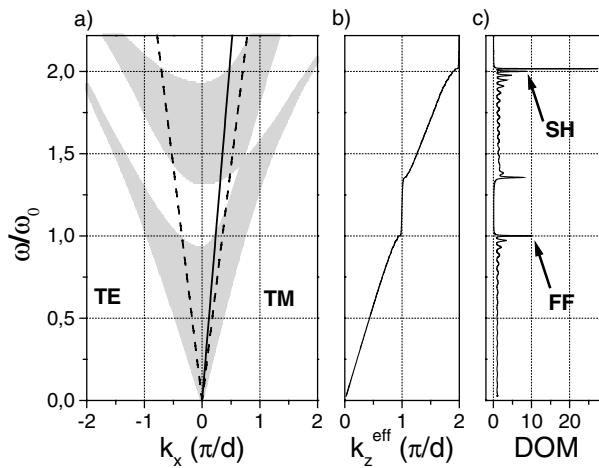


FIG. 1. (a) Projected band structure, light line, and direction of incidence, (b) effective dispersion relation, and (c) density of optical modes of the studied 1D-PC. The arrows indicate the fundamental and second harmonic operating positions.

that the real structure is represented by an effective homogeneous medium [6]. The  $k_x$  component is automatically phase matched due to the in-plane translational symmetry [11] and only the projection  $k_z^{\text{eff}}$  needs to be artificially phase matched. Figure 1(b) presents the effective dispersion relation  $\omega(k_z^{\text{eff}})$  at the angle of incidence  $\theta_i$  with  $k_z^{\text{eff}}$  calculated by taking into account the total phase  $\varphi_t$  accumulated by the field during its propagation through the finite structure:

$$k_z^{\text{eff}}(\omega) = \frac{1}{L} \varphi_t(\omega) = \frac{1}{L} \arg(t), \quad (1)$$

where  $t$  is the complex transmission coefficient. For a periodic structure with two different input and output media,  $\varphi_t$  must be derived numerically [12]. As seen in Fig. 1(b) the two plateaux of  $k_z^{\text{eff}}$  in the dispersion relation (band gaps) allow the compensation of the natural chromatic dispersion and the implementation of the phase-matching condition  $k_z^{\text{eff}}(2\omega) = 2k_z^{\text{eff}}(\omega)$ . This occurs, as indicated by the arrows in Fig. 1(c) for the first peak in the density of optical modes (DOM) of the first order gap and the second DOM peak of the second order gap. The DOM is defined as the inverse of the group velocity ( $v_g$ ), normalized to the value for an homogenous and infinite layer having the properties of the nonlinear material:

$$\text{DOM}(\omega) = \frac{\partial k_z^{\text{eff}}}{\partial \omega} = \frac{1}{v_g}. \quad (2)$$

Physically, the DOM is closely related to the strength of the optical field variation due to the 1D-PC feedback effect. A small group velocity corresponds to an increased DOM and to the achievement of a substantial increase of the interaction time between the fundamental and second harmonic (SH) waves. The unique advantage of 1D-PCs is that the spectral regions where both the DOM enhance-

ment and phase matching occur are nothing but the transmission peaks situated very close to the edges of the Bragg stop-band.

A major problem for the realization of such a 1D-PC in semiconductors, is that the index contrast between the constitutive layers should be high enough to compensate for the chromatic dispersion. This is a strong limiting factor for the use of common epitaxially grown III-V materials as linear layers in the 1D-PC, at fundamental wavelength shorter than  $3 \mu\text{m}$ . Because of the small refractive index contrast, phase matching remains inaccessible in GaAs/AlAs stacks and only the field enhancement effect was observed in our earlier experiments [4]. In this Letter, by oxidizing the AlAs layers into  $\text{AlO}_x$ , we have been able to reach a perfectly phase-matched operation. Oxidation overcomes the problem of the poor refractive index contrast and takes benefit of the low dispersion properties of  $\text{AlO}_x$ , while maintaining the advantage of monolithic growth.

Several structures were grown by low-pressure metal organic vapor phase epitaxy on [001] GaAs substrate. A typical structure consists of 18 periods of 151 nm of  $\text{Al}_{0.31}\text{Ga}_{0.69}\text{As}$  for the nonlinear layer ( $d_{14} = 108 \text{ pm/V}$ ) and 119 nm of AlAs. After the deposition of a silicon nitride mask defining different mesa lateral sizes (diameters of 25, 35, and  $55 \mu\text{m}$ ), chloride RIE is used to define cylindrical pillars. Finally, the lateral oxidation of the AlAs layers is carried out in a wet  $\text{H}_2\text{O} + \text{N}_2$  atmosphere at  $400^\circ\text{C}$ . The oxidation rate is  $55 \mu\text{m}/\text{hour}$ . The structure was designed for operation at an external angle of incidence of  $\theta_i = 42^\circ$  with respect to the stack axis at a fundamental wavelength of  $1.54 \mu\text{m}$ . At these wavelengths the refractive indices are  $n^{\text{AlGaAs}}(\omega) = 3.23$ ,  $n^{\text{AlGaAs}}(2\omega) = 3.46$ , and  $n^{\text{AlO}_x} \sim 1.5$ , both at the fundamental and the SH. Note that the coherence length corresponding to bulk AlGaAs is  $L_c = \pi/\Delta k_z = 1.64 \mu\text{m}$  where  $\Delta k_z$  is the projection of the phase mismatch onto the  $z$  axis. The curves shown in Fig. 1 correspond to the characteristic of our structure with the values of  $\text{DOM}_\omega = 10.2$  and  $\text{DOM}_{2\omega} = 8.4$  at the operating wavelengths.

The SHG experiments are performed using the pulses emitted by a  $1.48$  to  $1.58 \mu\text{m}$  tunable 76 MHz repetition rate optical parametric oscillator as the fundamental field. They are focused on the mesas by a  $20\times$  microscope objective. Pulse duration and incidence angle are 150 fs and  $42^\circ$ , respectively. The spectral bandwidth of a pulse is  $\sim 23 \text{ nm}$ . Because of the incidence angle, the spot is elliptic with a short axis of  $15 \mu\text{m}$ . Both mesas and the spot are visualized thanks to an IR camera. SH is collected via a multimode silica fiber with a core diameter of  $50 \mu\text{m}$ , located at  $\sim 200 \mu\text{m}$  above the mesa. The fiber is coupled to an optical spectrum analyzer with the bandwidth resolution set to  $0.5 \text{ nm}$  in order to measure the wavelength dependence of the generated SH.

Figure 2 represents the spectrum of the SH generated in reflection (thin full lines), for several fundamental central

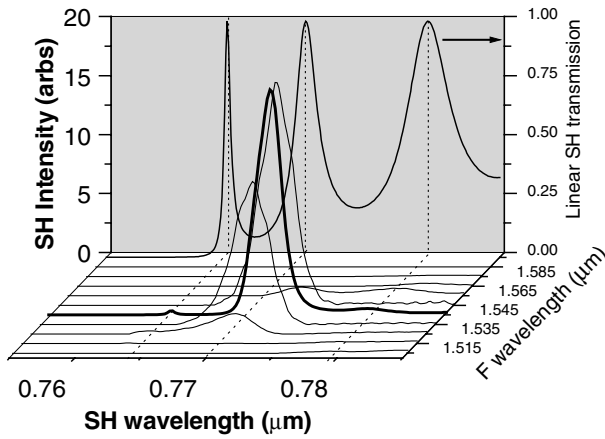


FIG. 2. Second harmonic intensity as a function of its wavelength (thin full line) for different fundamental central wavelengths (steps of 10 nm). The thick line corresponds to the calculated result at phase matching and agrees well with the measured spectrum for a fundamental central wavelength of 1.54  $\mu\text{m}$ . The transmission spectrum at the second harmonic is represented in the back of the figure (full line). The dotted lines correspond to the maxima of the transmission spectrum at second harmonic wavelength and clearly show that maximum SH intensity is obtained at the second transmission peak at the right side of the band gap.

wavelengths (steps of 10 nm). The background panel corresponds to the transmission spectrum of the stratified structure in the vicinity of the SH frequency (full line) and clearly shows the transmission resonances of the 1D-PC. The strongest SH is obtained for the second peak, the one taking advantage of both phase-matching and enhancement of DOMs at fundamental and SH.

We performed a nonlinear theoretical analysis based on the transfer matrix formalism under the approximation of an undepleted fundamental field, taking into account the full vectorial character of the nonlinear interaction [13]. The result, presented in Fig. 2 in a thick full line for the optimal central fundamental wavelength of 1.54  $\mu\text{m}$ , is in fairly good agreement with the experimental result obtained for the same fundamental central wavelength, corroborating the main 1D-PC effects.

The maximum conversion achieved displays an overall efficiency of 0.1% for a mean power of the fundamental of 90 mW (corresponding to a peak power of 8 kW), a rather promising value considering the modest length of the 1D-PC of 4.9  $\mu\text{m}$ . The internal conversion efficiency is estimated to be 0.35%. The difference between internal and overall conversion efficiency is mainly due to the spectral filtering of the incident pulse.

The present experimental demonstration raises the question of increasing the conversion efficiency to a level that would make band-edge phase matching competitive with other mechanisms. A simple analytic model, based on the coupled mode approximation and assuming identical input and output media (in particular, air), shows that in the limit of a large number ( $N$ ) of unit cells the efficiency is

expected to grow with the sixth power of  $N$  [7]. A numerical calculation using the physical parameters of our system shows that in the range of  $N$  values investigated, the growth of the SH intensity follows a  $N^{5.8}$  law (Fig. 3 full line).

In order to check this result we processed and tested additional structures having 10 and 28 periods. The SH intensity generated by the 10-, 18-, and 28-period samples was measured with the help of a fiberoptic laser delivering 8-ps pulses with a spectral width of FWHM  $< 0.4$  nm and a spatial extension of the order of a mm. This spectral width is narrow enough to avoid any spectral filtering by the band-edge resonance, while the pulse duration is long enough to reach a quasistationary regime (as assumed in the simulation) and to have a direct comparison of efficiencies. The experimental results, normalized to the 10-period structure, represented by the solid circles (dashed line), are very close to the  $N^{5.8}$  expected behavior. Although it is difficult to verify a power law with only three experimental points, our data indicate that the SHG efficiency does not grow any slower than  $N^{5.3}$ , far better than the quadratic dependence on the propagation length obtained in bulk or quasi-phase matching structures (see dot-dashed line).

The length of the nonlinear material of the 10-, 18-, and 28-period structures is, respectively, 0.9, 1.7, and 2.6 times the bulk coherence length  $L_c$ . Although these lengths are at best a few times  $L_c$ , we believe that the demonstration of the phase-matched operation in Fig. 3 is conclusive for two reasons. First, a calculation that takes into account the benefit from DOM enhancement but assumes a mismatch associated with  $L_c$  gives SH intensities that are lower by more than 1 order of magnitude than those measured in

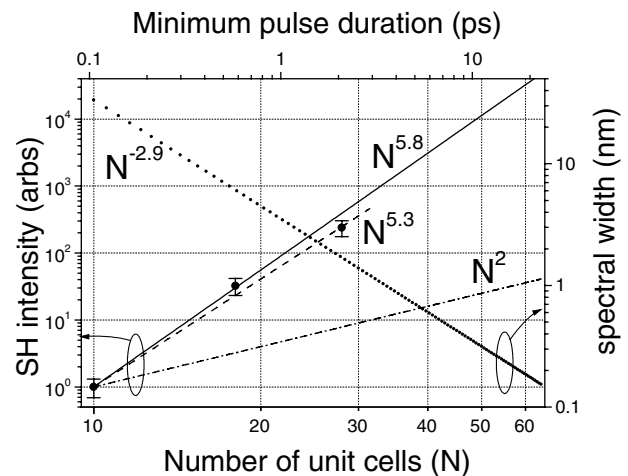


FIG. 3. Second harmonic intensity, normalized to the value of the 10-period sample, as a function of the number of 1D-PC unit cells  $N$  (left axis). The circles and dashed line correspond to the experimental results and best fit, respectively. The full line is the theoretical prediction, whereas the usual quadratic law is represented by the dot-dashed lines for comparison. The dotted line is the calculated spectral width of the fundamental transmission resonance (right axis).

our experiments on the 18- and 28-period structures. Second, in contrast to phase matching in the bulk, in which a mismatch  $\Delta k_z$  can be compensated geometrically in a short sample when  $\Delta k_z < 1/L$ , the discrete phase matching of 1D periodic media is independent of the length of the sample since the phase shifts introduced in the lateral resonances depend only on their order and is independent of  $N$ . Thus, the first lateral resonance of the fundamental stop-band can phase match only with the second lateral resonance of the second order stop-band as confirmed by our results shown in Fig. 2. In the same figure we see that the first and third resonances of the second order stop-band are never phase matched, independent of the length of the sample.

The increase of the conversion efficiency with the number of periods, however, is expected to meet several limitations as  $N$  increases. The most obvious comes from the reduction of the spectral width of the lateral resonances. Also represented in Fig. 3 (upper axis) is the minimum duration for the fundamental pulse allowed by the spectral bandwidth of the first lateral resonance of the 1D-PC. This duration can be deduced from the graph that gives the spectral width of that resonance as a function of  $N$  following a  $N^{-2.9}$  law represented by a dotted line (right axis). The second peak at the right side of the second gap, used for the SH, follows the same law, and its FWHM is smaller as needed for optimal conversion. As an example, for  $N = 55$ , a 15- $\mu\text{m}$ -long structure, the 1D-PC spectral bandwidth of 0.25 nm is still compatible with pulses as short as 15 ps. In that case the predicted conversion efficiency is 10% for a fundamental field peak power of 1 kW. Further increase in the number of periods gives rise to pump depletion and spatial walk-off and increases the role of sample imperfection. All these features are expected to reduce the efficiency slope. It is beyond the scope of this Letter to analyze in detail such limiting factors and their effects on the efficiency. Nevertheless, the strong departure from the usual quadratic law, expected theoretically and experimentally demonstrated in this Letter, allows a lot of room for the improvement of conversion efficiency.

In conclusion, we demonstrated experimentally SHG under a condition of discrete phase matching associated with the Bragg transmission peaks of a AlGaAs/AlO<sub>x</sub>

1D-PC at the fundamental and second harmonic wavelength. In addition to the phase matching condition, field enhancement that is obtained at these lateral resonances gives rise to a second harmonic efficiency growth close to the sixth power of the total length of the 1D-PC. This spectacular performance is nevertheless limited by the spectral filtering inherent in these structures which imposes a minimum duration for the fundamental field pulses of the order of 15 ps for a 55-period structure, for example. Implementation of wave guiding in 1D-PC would further increase the conversion efficiency because of strong transverse confinement and an increased interaction length. Finally, we note that this phase-matching approach could be extended to any second order nonlinear process.

We acknowledge Robert Kuszelewicz, Rama Raj, and Kamel Bencheikh for many helpful comments. This work was partially supported by OPEN ESPRIT Project ANLM.

- 
- [1] J. A. Armstrong, N. Bloembergen, J. Ducuing, and P. S. Pershan, *Phys. Rev.* **127**, 1918–1939 (1962); M. M. Fejer, G. A. Magel, D. H. Hundt, and R. L. Byer, *IEEE J. Quantum Electron.* **QE-28**, 2631–2654 (1992).
  - [2] N. Bloembergen and A. J. Sievers, *Appl. Phys. Lett.* **17**, 483 (1970); J. P. van der Ziel and M. Ilegems, *Appl. Phys. Lett.* **28**, 437 (1976); A. Yariv and P. Yeh, *J. Opt. Soc. Am.* **67**, 438 (1977).
  - [3] J. Trull, R. Vilaseca, J. Martorell, and R. Corbalan, *Opt. Lett.* **20**, 1746 (1995); A. V. Balakin *et al.*, *Opt. Lett.* **24**, 793 (1999); Golovan *et al.*, *JETP Lett.* **69**, 300 (1999).
  - [4] Y. Dumeige *et al.*, *Appl. Phys. Lett.* **78**, 3021 (2001).
  - [5] M. Scalora *et al.*, *Phys. Rev. A* **56**, 3166 (1997).
  - [6] M. Centini *et al.*, *Phys. Rev. E* **60**, 4891 (1999).
  - [7] C. De Angelis *et al.*, *J. Opt. Soc. Am. B* **18**, 348 (2001); D. Pezzetta *et al.*, *J. Opt. Soc. Am. B* **18**, 1326 (2001).
  - [8] C. Simonneau *et al.*, *Opt. Lett.* **22**, 1775 (1997).
  - [9] P. Yeh, A. Yariv, and C. S. Hong, *J. Opt. Soc. Am.* **67**, 423 (1977).
  - [10] Y. Fink *et al.*, *Science* **282**, 1679 (1998).
  - [11] Y. R. Shen, *The Principles of Nonlinear Optics* (John Wiley, New York, 1984).
  - [12] J. M. Bendickson, J. P. Dowling, and M. Scalora, *Phys. Rev. E* **53**, 4107 (1996).
  - [13] N. Hashizume *et al.*, *J. Opt. Soc. Am. B* **12**, 1894 (1995).